

# **Investigation of Muon Interaction with Colloid Suspension**

**P. Claiden<sup>1</sup>, S.D. Li<sup>2</sup>, J. Ren<sup>2</sup>**

**<sup>1</sup> School of Engineering, Sino-British College, Shanghai. <sup>2</sup> School of Engineering, Liverpool John Moore's University**

## **Executive Summary**

A type of detector is proposed with the aim of reducing the cost and size of systems capable of detecting nuclear contraband in shipping containers and lorries. In principle the device is capable of detecting a number of particulate radiation including neutrons. However this work concentrates on Cosmic ray Muon Scattering Tomography (CMST). Advantages of this technique include the passive nature of cosmic ray muons and their ability to penetrate and transverse large amounts of material. Conventional methods of muon detection such as gas scintillator tubes (GST) are expensive and bulky and a large detector volume is required. The proposed detector has a simple design based on a colloid suspension of electrically charge nanoparticles. In this work the benefits are explained, a theoretical analysis is undertaken and a proof of principle device built. Theoretical and experimental results are compared and appear to be consistent.

## **1.0 Introduction**

A type of particle radiation detector is proposed in which the particle interacts with nanoparticles in colloid suspension. The nanoparticles each have the same electrical charge so they are mutually repellent and therefore electrostatically stabilized. Depending on the type of radiation, interaction with nanoparticles may be columbic or direct collision. In either case the nanoparticle is perturbed from its equilibrium position and produces an electric field. This electric field is detected by an electrode array which is immersed in the colloid suspension. Because the mass of nanoparticle is known, the energy of the particulate radiation can be inferred from the amplitude of the electrical signal it produces.

This pilot project concentrates on the detection of muons (same charge as the electron), which could be part of future systems to use Cosmic ray Muon Scattering Tomography (CMST) to intercept nuclear contraband in shipping containers and lorries. However, in principle other types of radiation can be detected including neutrons, this raises the

intriguing possibility of a combined detector which distinguishes between types of radiation based on signal output and tracking data.

This pilot project is to prove principle of operation of the detector to negatively charged muons. Towards this end, a proof of principle device was built based on an existing prototype. The device was tested using a number of methods. These included: comparing possible muon signals with a theoretical analysis of the detector operation, testing with different frequencies of laser light to induce photo-emission of electrons ( $e^-$ ), testing with beta radiation sources ( $e^-$ ). The results were consistent with an electric field being generated by perturbed nanoparticles. The electron sources were able to provide data without having to wait for cosmic muon events. Responses to these electron sources were similar to the theoretically predicted muon response, and the nanoparticles appeared to return to electrostatic equilibrium when the source was removed. However voltage-time profiles were different because the source of electrons continues to perturb the nanoparticles in a way that the single muon interaction does not.

Future testing will correlate possible muon detection with a time synchronized Geiger counter capable of measuring GeV energies. The proof of principle device will also be exposed to a neutron source. Future technical development will concentrate on scaling-up the detector to  $m^2$  dimensions and on miniaturisation of electrode array circuitry with a higher packing density of electrodes.

## **2.0 Cosmic ray Muon Scattering Tomography (CMST)**

Cosmic ray Muon Scattering Tomography (CMST) is a technique that is being studied as a method for obtaining a profile of material densities within an enclosed volume. Cosmic ray muons passing through the enclosure will tend to scatter at angles that have a correlation with material density. For example there will be more scattering when muons pass through the structural materials than through voids within the enclosure. Two muon detectors are mounted in parallel either side on the container under investigation. Detection of muon tracks allows a profile of the distribution of materials to be inferred. Muon tracks through impeding material are compared to unimpeded tracks. The difference in track angle indicates the presence of denser materials. Advantages of this technique include the passive nature of cosmic ray muons and their ability to penetrate

and transverse large amounts of material. Systems based on this principle have already been developed to detect high density materials such as concealed uranium and plutonium. However conventional methods of muon detection such as gas scintillator tubes (GST) or gas wire detectors (GWD) are expensive and bulky; a large detector volume is required. Such detector systems are even larger if it is required to measure momentum as well as tracking position; absorbers or magnets are necessary.

### **3.0 Aims and Objectives**

In essence the idea is to reduce the size and cost of radiation detectors, and muon detectors in particular. A new type of detector is proposed based on interaction between radiated particles and a colloid suspension of nanoparticles. This pilot scheme is intended to prove the principle of operation of the proposed detector. A proof of principle detector was produced for this project, based on a previous prototype design. The prototype showed feasibility of the detection method and these initial results are included in the theoretical analysis which forms part of the verification procedure.

### **4.0 Proposal Details**

The new type of detecting element will be based on a different physical principle to gas scintillator tubes or gas wire detectors. Cosmic muons will interact with nanoparticles suspended in a colloid liquid. Each nanoparticle has the same amount of electric charge, and the same type of charge positive or negative. The nanoparticles are therefore mutually repellant and in an electrostatically stable suspension. When there is coulombic interaction between nanoparticle and muon, the nanoparticle moves from its equilibrium and produces an electric field. This electric field is detected by insulated electrodes within proximity of the interaction. The electrodes provide an electrical output that can be amplified and recorded.

A proof of principle device has been built. This consists of a thin layer (approximately 1.0 mm) of colloid suspension of negatively charged nanoparticles, covering an array of electrodes. Electrical output was recorded on six-digit voltmeters, one for each pair of electrodes in the array.

Nanoparticles may be for example (negatively charged) Silica or  $\text{Fe}_3\text{O}_4$  with sizes varying between 30nm to >5nm for example. The concentration of nanoparticles in suspension is approximately 30% by volume. The effect of nanoparticle concentration and size on sensitivity of the detector is explained in Section 7.1.

Surface charge on the Silica nanoparticle is maintained by the correct (alkaline) pH of the electrolyte i.e. liquid part of the colloid suspension.

## **5.0 Benefits**

In the proof of principle detector, electrode separation distance is approximately 1.2mm. Potentially this distance reduces to microns if micro-machining is used to make the electrode array. By way of comparison, the diameter of the gas scintillator detector (GST or GWD) is a minimum of approximately 1 cm. Closer packing of detecting elements, improves resolution of the detector. Thus it is possible to measure smaller angular deviation and achieve greater discrimination between material densities and shapes.

Also, GST and GWD are  $\approx 1.0\text{m}$  long compared to the millimeter (thick) dimensions of the proposed detector. Hence volume of the device will be considerably reduced, making it portable and easier to deploy.

One of the main benefits of the colloid detector is cheap materials, and low manufacturing costs due to a simple design. Most of the cost of the colloid detector will be incurred in manufacture of addressable electrode arrays, which will be required at later stages of development. However, the technology for this is commercially available at present with pixel image sensing as used in mobile phone cameras.

In the colloid detector, mass of the nanoparticle is known so muon momentum can be calculated directly from electrode signals. Muon momentum provides information in addition to scattering angle. For example, a higher momentum muon-track from an object with the same scattering angle as other objects would indicate that particular object is denser.

In the colloid detector, electrical supply is only necessary for amplification and recording so there is low power requirement compared to existing detectors. For example, high voltage sources are needed for both gas scintillator tubes and gas wire detectors.

## **6.0 Proof of Principle Device**

The proof-of-principle device was based on the design of the existing prototype. The device includes 4 pairs of electrodes with 1.2mm inter-electrode spacing. The electrode array is enclosed in a liquid tight container and mounted on a printed circuit board. Voltage measurements were taken across each pair of electrodes using Six-Digit Tektronix DMM 4050 voltmeters capable of measuring  $10^{-5}$  volts. In the proof of principle device the colloid suspension contained 30 nm (average) diameter silica nanoparticles which were surface functionalized by triethoxypropylammonisilane and supplied by Sigma-Aldrich Co. The concentration of nanoparticles was 30% by volume.

The area of the electrode array is approximately 6mm x 32mm i.e. with area  $192\text{mm}^2$ . Thus, if the cosmic muon background is assumed to be  $10^2$  muons/ $\text{m}^2\text{sec}$ , the proof-of-principle device should be able record an average of two muon interaction per 1000 seconds. It is important to note that the fully developed detector will have a surface area  $> 2\text{ m}^2$  with muons rate  $> 200$  per second passing through; much larger than the proof of principle device.

## **7.0 Proof of Principle Verification**

There were three methods used in this project to prove the principle of operation of the colloid detector. All show the effect of negatively charged particles on electrical output from the detector:

- 1) Compare possible muon signals from the detector with a theoretical analysis of the detector operation. Theoretical calculations show a (negative) voltage spike produced by a muon. The voltage-time profile of this spike was compared to results from the proof of principle detector
- 2) Expose the detector to different frequencies of laser light to induce photo-emission of electrons. UV and IR lasers are pulsed on to the surface of the colloid suspension and the electrical output is measured

- 3) Expose the detector to a beta radiation source. The Strontium 90 beta source used for this test had an activity of  $3.7 \times 10^6$  Becquerel which produced a rate of electron interaction far greater than the relatively rare cosmic muon events. It was possible to observe the detector response to negatively charged particles without waiting for the muon events.

### 7.1 Theoretical Analysis and comparison to detector output showing potential muon interaction

Simple conservation of energy concepts are used demonstrate feasibility of the colloid detector. The calculated results were then compared with prototype performance.

In the theoretical analysis the cosmic muon ( $e^-$ ) is assumed to pass through the center of the cubic lattice, equidistant from the nanoparticles; as shown in Figure 1. This simulates the weakest possible electrical interaction between muon and nanoparticle. Viscous damping is ignored and velocities are assumed to be in the  $-Z$  direction only i.e. no vector components.

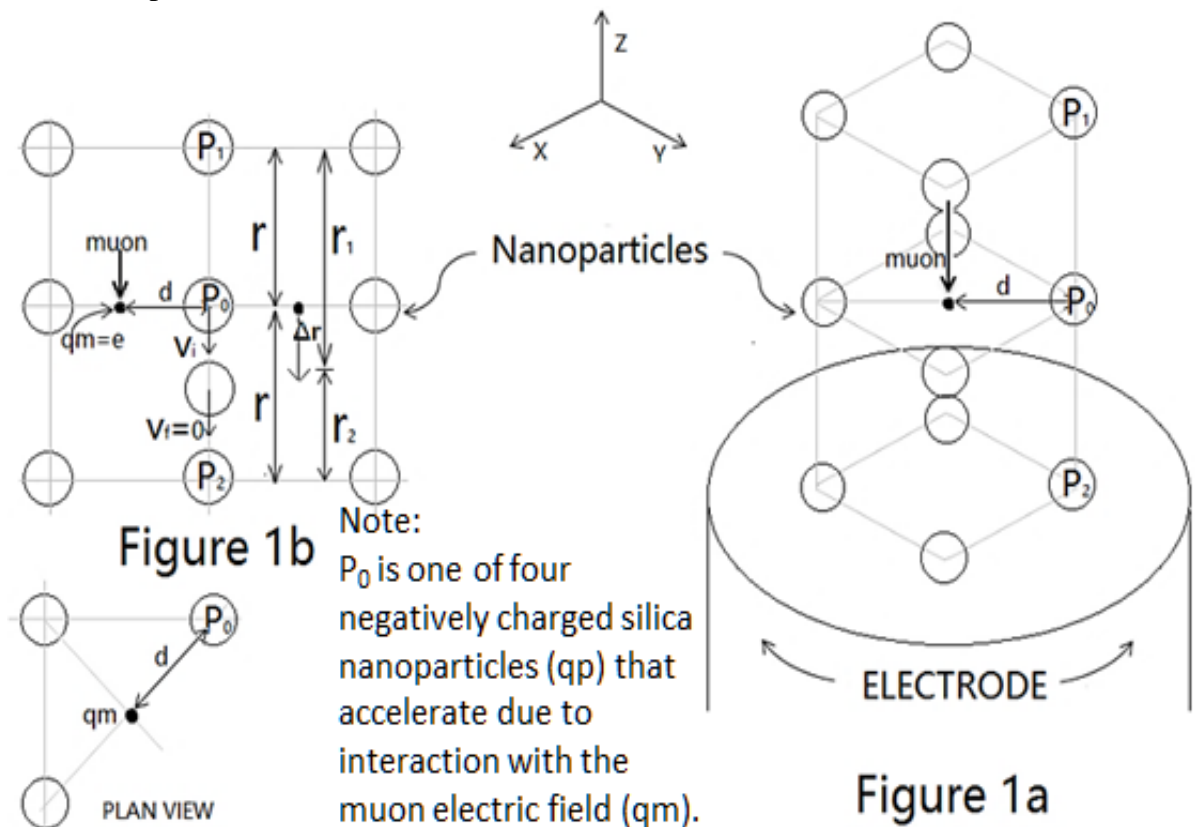


Figure 1 Assumed cubic lattice arrangement and dimensions for muon/nanoparticle interaction

Figure 1a shows an assumed cubic lattice arrangement of charged nanoparticles in electro-static equilibrium. Figure 1b shows dimensions of the lattice used in subsequent calculations. P<sub>0</sub>, P<sub>1</sub> and P<sub>2</sub> are illustrations of typical nanoparticles held in electrostatic equilibrium due to their mutually repellant negative surface charge. P<sub>0</sub> is perturbed by a distance Δr due to interaction with the muon electrical field.

Table 1 below shows the calculated Surface Charge and Mass for nanoparticles with diameters of 7nm and 30nm. Also shown are the calculated distance parameters r and d for the nanoparticles by assuming a 30% volume concentration in the colloid suspension.

Nanoparticle Diameter (nm)	Inter-particle distance (nm) r	Diagonal distance from muon to nanoparticle (nm) d	Charge on nanoparticle surface (C)	Mass of the nanoparticle (kg)
30	39	27.5	2.26 x 10 <sup>-19</sup>	2.18 x 10 <sup>-20</sup>
7	9.4	6.66	12.3 x 10 <sup>-18</sup>	2.76 x 10 <sup>-22</sup>

**Table 1 Calculated Inter-particle Distances and Distance from muon to nanoparticle, also Surface Charge and Mass of nanoparticles**

Subsequent calculations were based on parameters in the table and the following conservation equation:

$$\Delta K + \Delta U_e = \Delta k + q\Delta V = 0$$

Where: K is kinetic energy (J), U<sub>e</sub> is electrical potential energy(J), q is electric charge(C) and V is electrical potential (J/C)

Calculation of velocity is as follows:

$$\left(\frac{1}{2}mv_i^2 - \frac{1}{2}mv_f^2\right) + \frac{kqmqp}{d} - \frac{kqpqp}{\left(\frac{1}{r} - \Delta r\right) - \left(\frac{1}{r} + \Delta r\right)} = 0$$

Calculation of electrical potential is as follows:

$$\left(\frac{1}{2}mv_i^2 - \frac{1}{2}mv_f^2\right) + qp\Delta V = 0$$

Where:  $v_i$  and  $v_f$  are initial and final velocities of the nanoparticle (m/s).  $m$  is the mass of the nanoparticle (kg),  $k$  is the electrostatic constant for which the relative permittivity  $\epsilon$  of the fluid suspension is assumed to be 80. Other symbols are as indicated in Figure 1.

A numerical approach was used: Limiting values of  $\Delta r$ , when velocity was zero, were calculated first. Then  $\Delta r$  was divided into incremental amounts and other values of velocity, hence electrical potential were calculated. The results of voltage versus (calculated) times are shown in Figure 2.

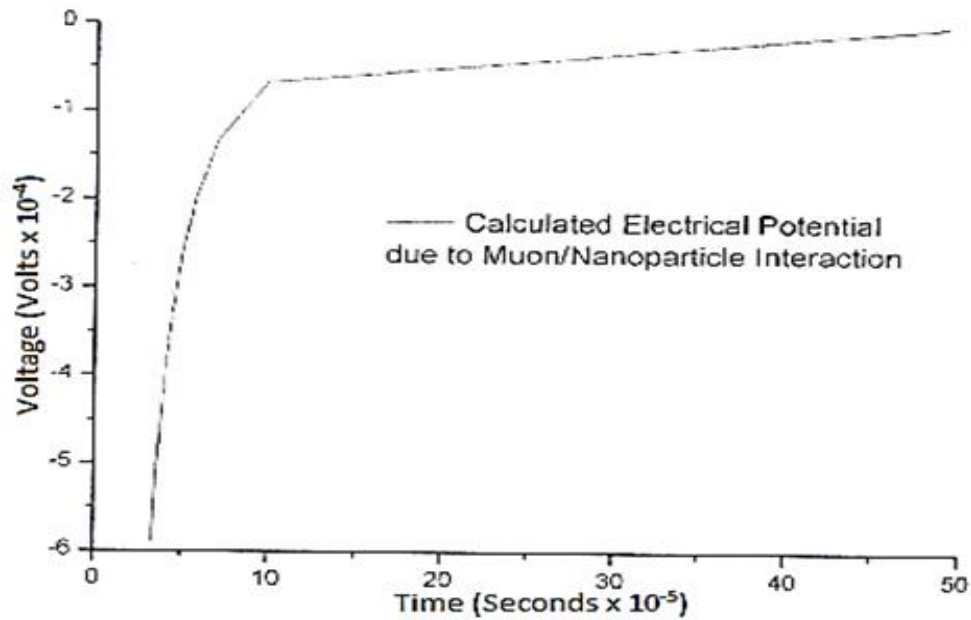


**Figure 2 Calculated Electrical Potential due to muon/nanoparticle interaction**



The values in Figure 2 may explain the trailing edge of the voltage-time profile of the spike shown in Figure 3; obtained from the prototype detector.

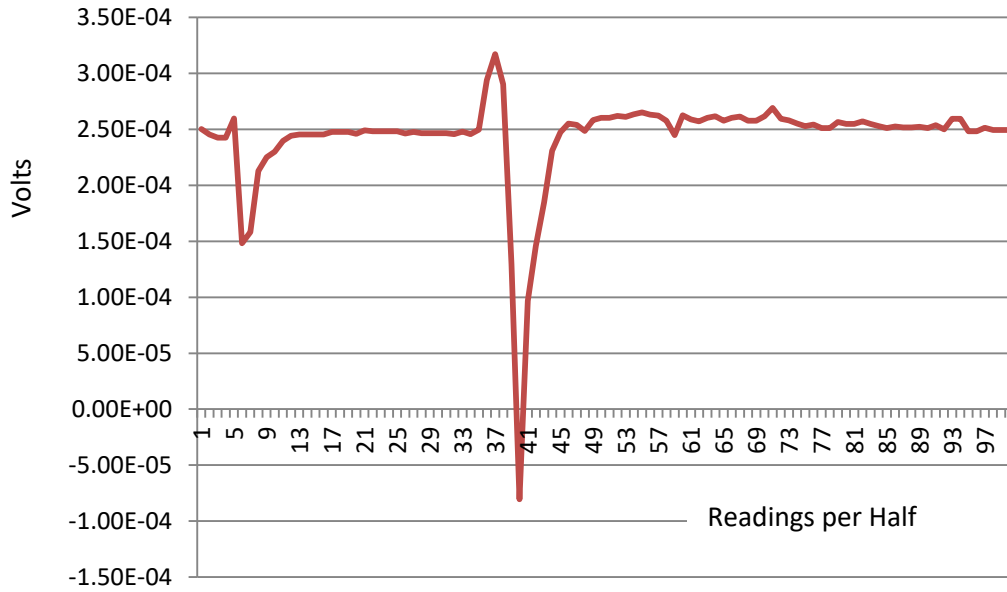


**Figure 3 Detector voltage-time profile, possibly showing interaction with Cosmic Muon during a 50 second recording period**

Similar spike profiles, possibly representing muon interaction, are also shown in Figure 4. This data was obtained by recording the output from the proof of principle device over a period of approximately 2000 secs. The number of spikes agrees with the prediction, made in Section 5, that there will be a mean muon interaction rate of approximately 2 muons per 1000secs.

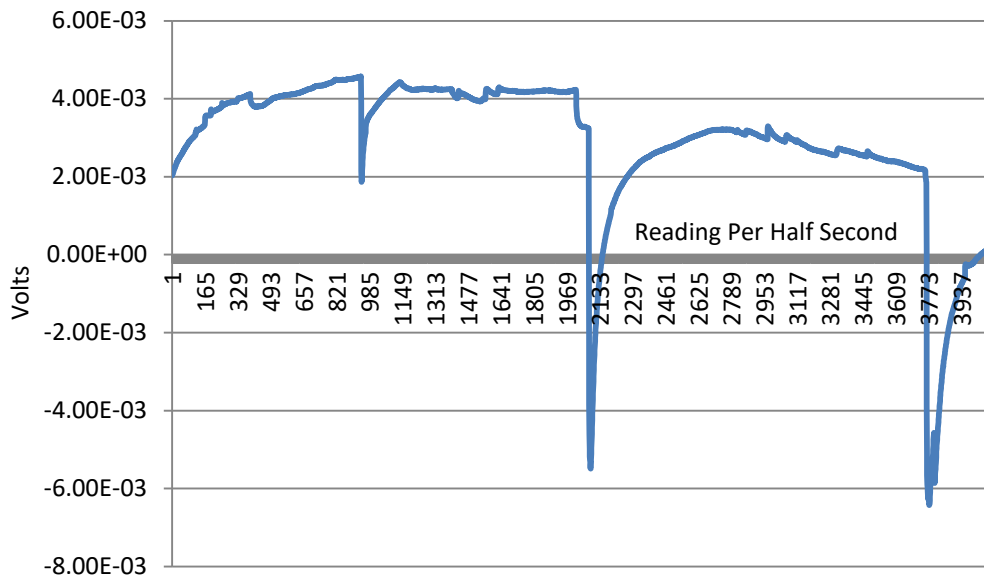


**Figure 4 Detector voltage-time profile, possibly showing interaction with Cosmic Muons. Recording period is 2000 seconds**

## 7.2 Prototype Testing using pulsed laser light

The prototype was tested using low power lasers. Photonic/nanoparticle interaction is different to the muon/nanoparticle columbic interaction. Electrons are ejected when photons interact with the nanoparticle through photo-emission. However the overall effect will be similar to muon interactions i.e. perturbed charge on the nanoparticle causes it to move from its equilibrium position. This movement and subsequent movement of other nanoparticles produce an electric field.

Tests were conducted using lasers  $<200$  mW output. To reduce light intensity further the prototype was covered with 0.31mm thick cardboard having 80%-90% obscuration. The lasers were manually switched on and off to produce arbitrary-pulsed illumination.

Figures 5 and 6 show the unamplified output from an electrode pair in the prototype. Figure 5 shows the maximum signal amplitude was  $\approx -1.5 \times 10^{-3}$  volts in response to IR (605 nm) and Figure 6 shows maximum signal amplitude  $\approx -2.5 \times 10^{-3}$  volts with UV (405 nm). The fact that signal amplitude depends on frequency suggests that detector is responding to electrons produced by photo-emission.

As a control experiment the laser light was shone on exposed copper electrodes. There was no electrical output.

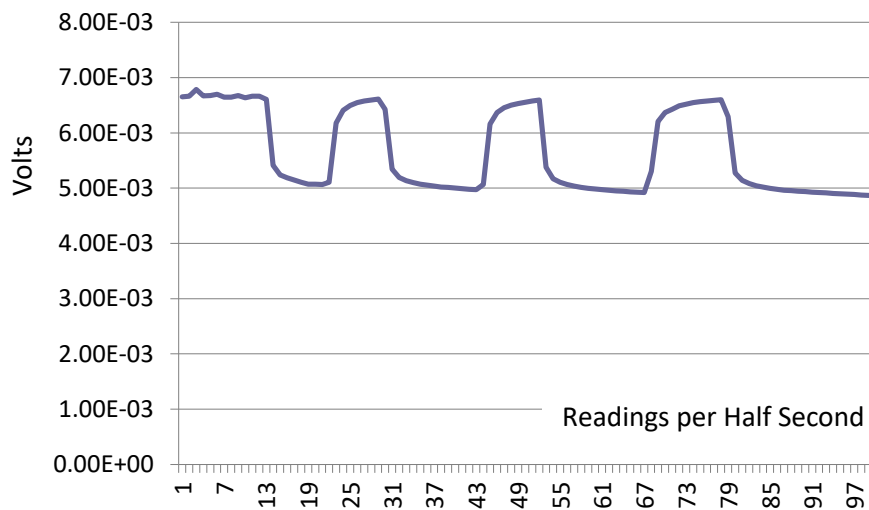


**Figure 5 Detector response to pulsed IR laser light at 605nm**

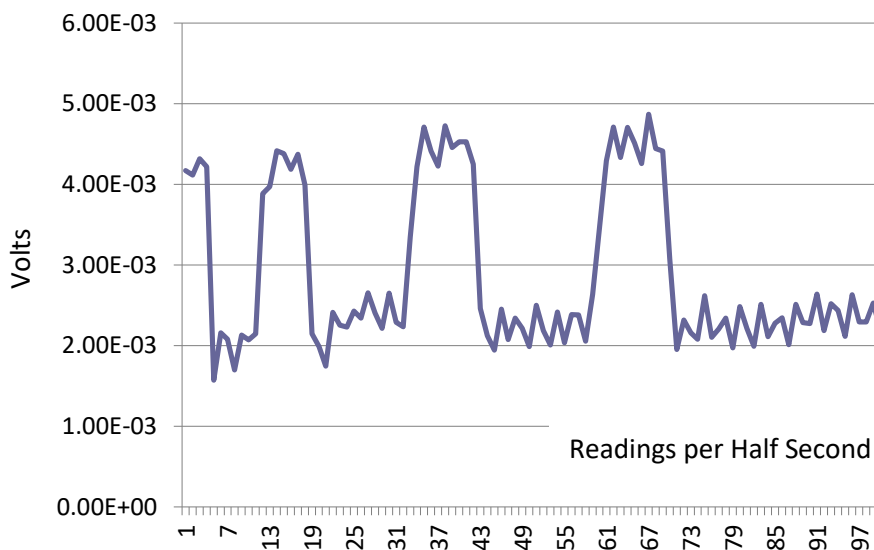


**Figure 6 Detector response to pulsed UV laser light at 405nm**

### 7.3 Prototype testing using Beta radiation source

Figure 7 shows the detector exposed to a Strontium 90 Beta source. Exposure was for arbitrary and manually timed intervals; between readings 6 and 14, between readings 21 and 36, between readings 86 and 96. These are approximately equivalent to time intervals of 4, 7 and 5 seconds.

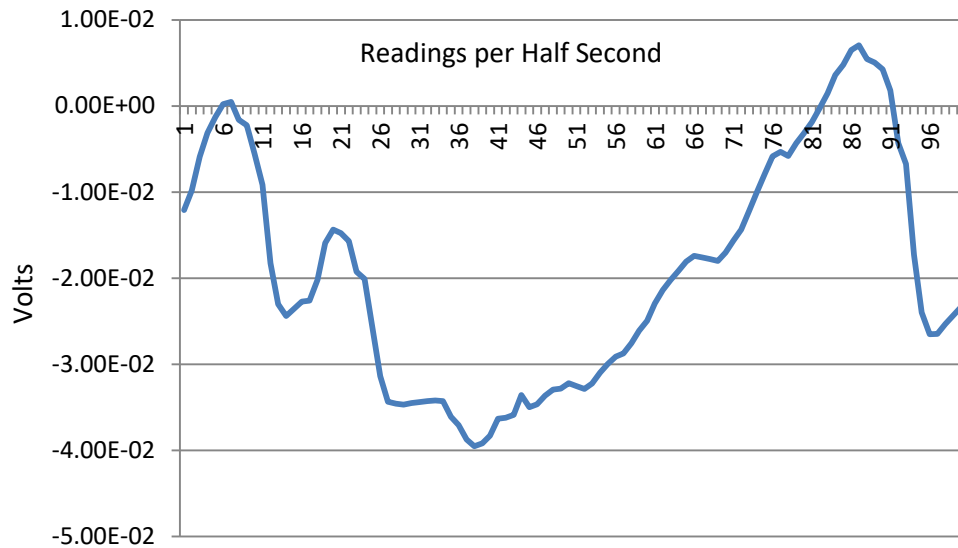


**Figure 7 Detector response to intermittent exposure to Strontium 90 Beta source**

Figure 7 shows the Beta source ( $e^-$ ) produces a negative electrical signal in response to application of the electron source. When the source is removed the nanoparticles return to equilibrium. This is consistent with the principle of nanoparticle interaction described in Section 7.1. However it is apparent that the continuous Beta source in Figure 7 effects the output in a way that the single muon event shown in Figures 3 and 4 does not. Consequently the voltage-time profiles were different in each case. The continuous source of lower energy (550KeV) electrons produces a shallower curve-gradient.

### 8.0 Future Development

Future testing will correlate possible muon detection and a time synchronized Geiger counter capable of measuring GeV energies. Also the proof of principle device will be exposed to a neutron source.

Future technical development will concentrate on scaling-up the detector to  $m^2$  dimensions, and on miniaturisation of electrode array circuitry with a higher packing density of electrodes. At some future stage, it is anticipated that a fully developed detector will be approximately 50 mm thick with a minimum area of  $2.0 m^2$ . Azimuth and altitude angles of the muon track will be obtained from two parallel detectors either side of the enclosure being inspected.

## **9.0 Conclusions**

A type of particulate radiation detector is proposed that measures the electric field generated when sub-atomic particles interact with a colloid suspension of charged nanoparticles. The electric field is generated when charged nanoparticles are perturbed from an electrostatic equilibrium position. A proof of principle device was produced and although in principle it should be capable of detecting neutrons and alpha particles (amongst others) this work concentrates on detection of muons. The voltage-time profiles of possible muon interactions were obtained using a theoretical analysis based on conservation of energy concepts. The theoretical predictions were consistent with results from the proof of principle detector showing possible muon events. In addition the device was tested by exposure to electron sources. Although not exact simulations of muon events, the electrons demonstrated the mechanism of coulombic interaction. An indirect electron source was obtained by illuminating the colloid suspension with pulsed laser light. The response of the detector was negative (below a positive datum) electrical pulses corresponding to the laser illumination. The fact that amplitude of the response depended on the frequency of the laser demonstrated that the electron source was produced by photoemission. The colloid suspension was also intermittently exposed to a continuous beta radiation source. The response was consistent with the electric field generated by perturbed nanoparticles but voltage-time profiles due to a continuous, relatively low energy electron source have shallow gradients compared to rare high energy events that are characteristic of muons.